Journal of Materials Science and Surface Engineering, 9(1): 1078-1085
ISSN (Online): 2348-8956; DOI: https://doi.org/10.52687/2348-8956/917

Peer Reviewed

Co-Precipitation Mediated Fabrication of Composite with MnS_2 and Reduced Graphene Oxide as Potential for Inactivation of Ortho-Nitrophenol and Pathogens

D. Varaprasad[1] · B. Sathish Mohan[2] · Dharmasoth Ramadevi[3-4] · K Basavaiah[1] · P. Vani[1]

[1]Dept of Inorganic & Analytical Chemistry, Andhra University, Visakhapatnam 530003, India.
[2]Bio Enviro Chemical Solutions, Visakhapatnam 530017, India.
[3]AU College of Pharmaceutical sciences, Andhra University, Visakhapatnam 530003, India.
[4]Samuel George Institute of Pharmaceutical sciences, Markapur, Andhra Pradesh 523316, India.

ABSTRACT
In this paper, the authors have report the fabrication of MnS_2 with reduced graphene oxide (MnS_2-RGO) composite through co-precipitation route. The prepared samples were characterized by analytical instruments like XPS, FTIR, XRD, BET, SEM-EDX, TEM, UV-DRS and TGA for understanding the optical, electrochemical, structural and thermal properties. The prepared composites and bare MnS_2 were examined for their photocatalytic performance by the degradation of *o*-nitrophenols under visible light irradiations. However, MnS_2-RGO-2 composite was the most effective photocatalyst for the degradation of *o*-nitrophenols in 75 min and can be recycled for continuous five cycles. The MnS_2-RGO composites and bare MnS_2 were further examined their antimicrobial activity over *E.coli, S.aureus, S.typhi and V.cholera*. In addition, the effect of RGO on enhanced catalytic degradation of *o*-nitrophenols under visible light irradiations and antibacterial activity as prepared composite exhibits tremendous properties of both MnS_2 and RGO.

ARTICLE HISTORY
Received 05-06-2022
Revised 15-06-2022
Accepted 24-06-2022
Published 08-09-2022

KEYWORDS
MnS_2-RGO
Co-precipitation
Ortho-nitrophenol
Photocatalytic Degradation
Antimicrobial Activity

Introduction

Advanced oxidation processes (AOPs) predominantly photocatalysis have raised a promising solution for the degradation of harmful organic pollutants and microorganisms in polluted water [1]. US EPA (Environmental Protection Agency) declared that 4-nitrophenol (4-NP) has been recognized as a non-biodegradable pollutant owing to its great solubility and stability in water media, also accumulated on the surface of the soil with no degradation [2]. 4-NP is carcinogenic and affects the CNS (central nervous system) that resulting in hormone imbalance and finally leading to kidney malfunctioning, eyes irritation and liver disordering [3]. Therefore, it is very important to develop an effective method to either modify or remove 4-NP before releasing it into the environment. Among various photocatalysts, the composites of reduced graphene oxide (RGO) with semiconductors are of significant relevance since they have suitable optical and physicochemical properties like solar light harvesting tendency, great stability, great photocharge separation efficacy and excellent adsorption of pollutants from aqueous solutions [4]. Graphene based materials have been extensively studied because of their remarkable bactericidal performance in broad applications in photocatalysis and antimicrobial activity [5-6]. Hence, RGO based composites can have greater photocatalytic efficacy towards the degradation of dye pollutants and pathogens removal. Recently, RGO based binary, ternary and quaternary composites have been developed over the last two decades [7-8]. The earlier reports mentioned the improvement strategy by metal or non-metal doping of RGO or semiconductor added to RGO (RGO/metal/semiconductor, RGO/bimetal oxides).

Semiconductor metal sulfides (MnS_2, ZnS) have been extensively used as photocatalysts, single electron transistors and solar cells [9]. Manganese sulfide (MnS_2) possesses wide bandgap energy of 3.7 eV and exists in three different forms [10]. This paper discusses the role of RGO loading on photocatalytic degradation of *o*-nitrophenols under visible light irradiations. Moreover, the possible mechanism of photocatalytic degradation of *o*-nitrophenols using the proposed MnS_2-RGO composite Furthermore, the plausible photocatalytic pathway for the generation of free radicals by RGO-based composites is also explained in detail. Also, study the inactivation of pathogens by prepared MnS_2 and its composites. This study will be beneficial to the researchers in field of materials science for developing new metal sulfides based RGO composites as superior photocatalysts and benign antimicrobial agents.

Experimental

Materials

Graphite flakes, sodium nitrate ($NaNO_3$), sulfuric acid (H_2SO_4), manganese chloride ($MnCl_2$), hydrogen peroxide (H_2O_2), ethanol (C_2H_5OH) hydrochloric acid (HCl), ammonium sulphate ($(NH_4)_2SO_4$), sodium hydroxide (NaOH), and sodium borohydride ($NaBH_4$) were procured from Sigma Aldrich Company, India and used without further purification. The *o*-Nitrophenol was received from Merck chemical Ltd, India, used without further purification and Milli Q water was used in all preparing solutions.

Methodology

Synthesis of desirable composite

Corresponding Author: B. Sathish, Tel: +91 7989524380
Email: bsathish401@gmail.com
Contents lists available at http://www.jmsse.in/ & http://www.jmsse.org/

In a facile synthesis of MnS_2-RGO composite, initially, the pre-weighed amount of GO was sonicated for 1h. In another beaker, the 40 mL of $MnCl_2$ (0.25M), 25 mL of ethanol and 30 mL of $((NH_4)_2SO_4$ (0.1M) were taken, allowing for 1h stirring. The GO was added to the above solution and a pinch of $NaBH_4$ was also added. This solution was mixed for 3h continuously with a controlled temperature of 90 ^oC. After completion of the reaction, the mixture solution was cooled to reach room temperature and then washed several times with ethanol followed by water. Finally, the obtained brown coloured product was filtered and dried overnight in a hot air stabilizer at 70 ^oC. In absence of GO, the MnS_2 nanoparticles were synthesized by following the same procedure.

Preparation of GO

Universal modified Hummer's method was adopted to obtain GO. For that, 3g of graphite flakes were sonicated for 30 minutes before oxidation. Then, sonicated graphite (1 g) and $NaNO_3$ (0.5 g) were suspended in 69 ml concentrated sulphuric acid in an ice bath (to maintain the temperature below 5 ^oC) in a 500 ml round bottom flask under gentle magnetic stirring for 15 min. Then 3 g of $KMnO_4$ was added continuously pinch by pinch by keeping the temperature of the solution did not exceed 20 ^oC. Then, the ice bath was removed and stirred the solution at 35 ^oC under a reflux condenser for 3 hours. After that, 130 ml of distilled water was added and stirring continued for an additional one hour. Excess unreacted $KMnO_4$ was removed by 10 ml of 30% H_2O_2. The complete removal of $KMnO_4$ was indicated by a colour change from dark to yellow. As prepared GO was carefully washed with deionised water several times and dried overnight in the oven at 70 ^oC.

Characterization

The prepared catalysts were further characterized using analytical instruments in a detail, microscopic studies were conducted on SEM and TEM to study morphology with elemental composition by EDX analysis. The crystallinity of the compound was studied using XRD patterns using Bruker AXS D8 Advance X-ray diffractometer with Cu-kα wavelength at the scan rate speed of 0.02^o/C. The functional groups on the catalyst surface were determined using FTIR analysis (IR prestige 21, Shimadzu) in the range from 500 to 4000 cm^{-1}. XPS (PHI 5000 versaprobe III) and UV-visible spectrophotometer (Shimadzu 2600R) were used to study the optical properties of prepared samples in the wavelength of 200 to 800 nm. TGA analysis was performed using TG100 with a scanning temperature of 28-1000 ^oC. BET analysis performed using BELSORP MiniII in presence of N_2 and He gas.

Dye degradation experiment

The photocatalytic performance of prepared samples (MnS_2 and MnS_2-RGO composites) was executed by experimenting with *o*-nitrophenol. A well-designated photoreactor with a visible lamp and magnetic stirrer was used for this purpose. The initially desirable concentration was prepared and the same was taken into a 250 mL beaker and the pre-weighed catalyst amount was added to it. The mixture solution is stirred for 30 min to optimize the adsorption of dye molecules on the surface of the catalyst. Then, light is allowed and extends for more one and half an hour. The aliquots were collected at regular time intervals, which further allowed obtaining UV-Vis spectral analysis for measuring the degradation rate. The percentage of the degradation rate of *o*-nitrophenol was measured through A_t-A_o/A_t x 100 here, A_t and A_o are the absorbance at a time 't' and initial time of *o*-nitrophenol solution respectively.

Antibacterial activity

The Bacterial cultures are grown overnight at 37^{o}C temperature were used for testing the antibacterial activity. Nutrient agar medium (High media) was dissolved in the water this was distributed in a 100ml conical flask and was sterilized in an autoclave at 121^{o}C 15lbp for 15min after autoclaved the media poured sterilized petriplates. Chloramphenicol was taken as a positive control for antibacterial activity. The antibacterial activity of the compound was evaluated by Agar well diffusion method (Perez et al., 1990). Inoculums were spread over the surface of agar plates with a sterile glass spreader. Four wells were made at an equal distance using a sterile cork borer. To examine the antibacterial activity of the compounds were made final concentrations of 40mg/ml, 60µg/ml, 80µg/ml of extract were poured on each well and then plates were incubated for a period of 24h at 37^{o}C in an incubator after incubation diameter (mm) of the clear inhibitory zone formed around the well was measured.

Results and Discussion

XRD spectral analysis

Fig.1 displays the XRD patterns of prepared MnS_2 and its composites with RGO (MR-1 and MR-2 composites). Noticed in the XRD spectrum of GO that a sharp peak was noticed at (2θ) 11^o which signifies the (001) plane of GO [11]. But, the same peak is not presented in MR composites may be due to its transformation into another. Probably, GO might be converted into RGO because a reducing agent (sodium borohydride) was used during the synthesis of composites. Besides GO, the other XRD spectra (MnS_2 and MR composites) have shown the XRD patterns of 23.2^o, 32.6^o, 36.2^o, 44.3^o, 60^o, and 64.6^o with the confirmation from standard JCPDS (File No.25-0549). Debey-Scherrer's equation was used in this study to measure the average crystalline size (S) of prepared samples.

$$S = k\lambda / \beta\cos\theta \qquad (1)$$

Where 'k' is the scherrer's constant usually taken as 0.94, 'λ' denotes the X-ray wavelength, 'β' is the full width at half maximum (FWHM) and 'θ' denotes the diffraction angle. The composites showed a greater effect on the size of the prepared MR composites, a significant amount reached by RGO loading. MR-1 composite was found to be 21.3 nm and 21.2 nm for MR-2 composite. In general, the size of the composite contributes more effectively to the greater photocatalytic performance of prepared samples. Lesser sized samples usual have a higher surface area that can accommodate more adsorbent species on their surface. Moreover the impact of the preparative approach, composite formation and morphology lie in the extent of better catalytic efficacy [12].

XPS analysis

In connection with EDX results, XPS analysis was further performed in this study to explore the elemental consistency of prepared samples. The obtained results are well-matched with previous reports [13]. The EDX results confirmed that the surface of the prepared MR composite contains the elements of Mn, S, C, O and the respective

peaks of XPS analysis reported binding energy of 640 and 652, 168, 283 and 529 eV respectively as shown in Fig.2 [13].

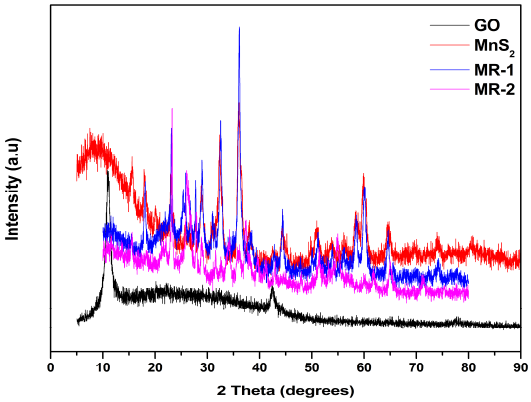

Figure 1: XRD patterns of prepared MnS_2 and its composites with RGO

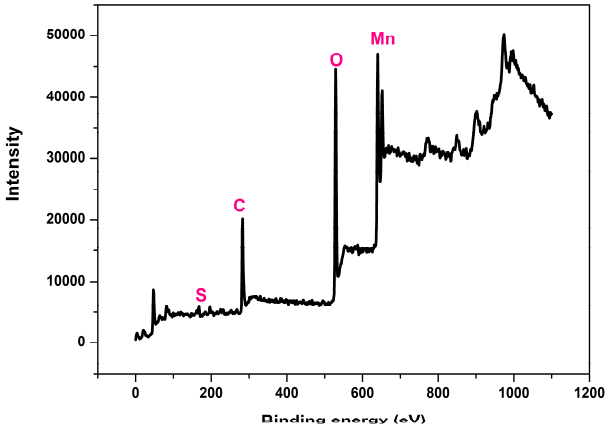

Figure 2: XPS spectrum of prepared composite MnS_2-RGO

FTIR study

Fig.3 shows the FTIR spectral analysis of prepared samples (MnS_2 and MR composites prepared by co-precipitation). The transformation of GO into RGO can be seen in the FTIR spectrum of GO by the peak of 3430 cm^{-1} (represents the O-H group of the hydrated molecule) disappearing in prepared MR composites. The SO_4^{2-}, C=C and C-O groups also noticed in prepared composites and the respective peaks located at 667, 1418 and 1090 cm^{-1} respectively [14-15].

BET analysis

The prepared samples (MnS_2 and MR composites) were further examined BET analysis under the N_2 sorption isotherm and the results are shown in Fig.4. BET analysis is performed for determine the surface area of prepared samples (MnS_2 and MR composites). The calculated BET surface area of prepared MR-2 composite was found to be 180 Va/cm^3. Which is higher than MR-1 composite (35 Va/cm^3) and MnS_2 (0.15 Va/cm^3). The results found that the desorption curve has a steep area with the closure of the H3-type hysteresis loop. The formation of RGO based composite with MnS_2 helps the increase in the surface area of prepared composite is evident from the agglomeration of RGO (SEM images) [7]. In addition, the MnS_2-RGO composite reached greater surface area results maximum degradation rate.

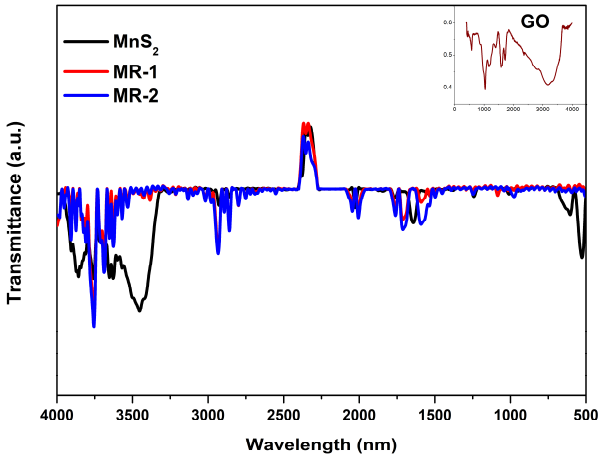

Figure 3: FTIR spectra of prepared samples with an inserted graph of GO

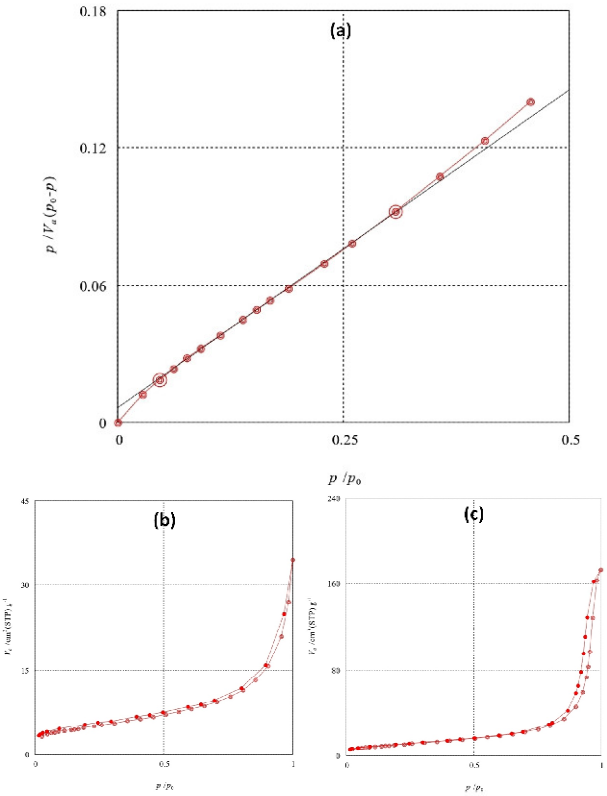

Figure 4: Adsorption-desorption isotherm of (a) MnS_2, (b) MR-1 and (c) MR-2 composite

TGA study

Thermogravimetric analysis (TGA) was performed in this study to reach out thermal stability of prepared samples (MnS_2, MR composites) at a heating range of 28 to 800 ^oC and the results are presented in Fig.5. We can easily distinguish the bare MnS_2 from its composites by endotherm peaks. The TGA curves of MnS_2 were 200 ^oC due to dehydration and 517 ^oC for complete turned into ash. However, the same occurred in both MR composites occurred at 252 ^oC and 600 ^oC respectively.

Optical properties analysis

The bandgap energy of prepared materials was determined using the Tauc plot equation as Eq 2.

$$\alpha h\upsilon = A\,[h\upsilon - Eg]n/2 \qquad (2)$$

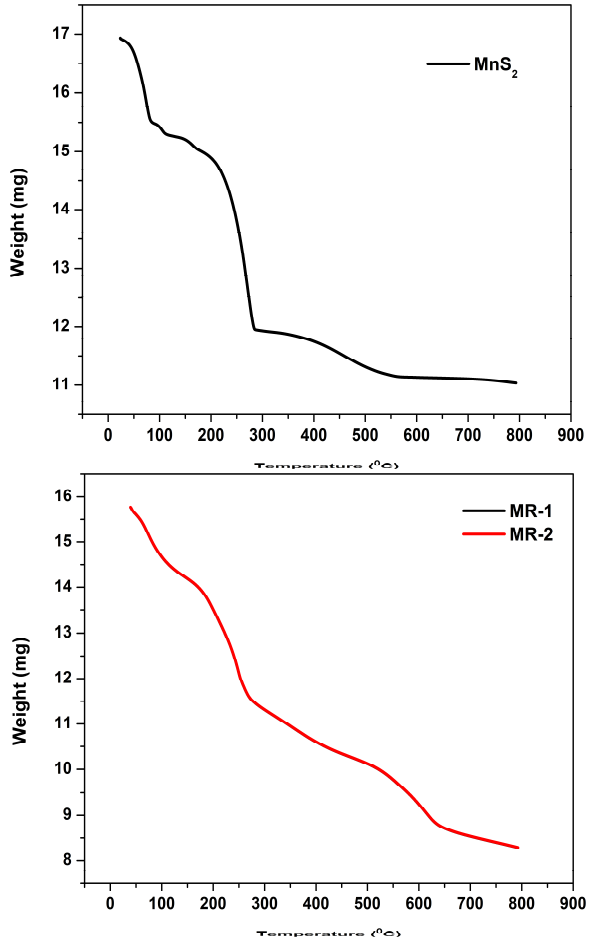

Figure 5: TGA images of prepared MnS_2 and MR composites

Where 'α' is the absorption coefficient, 'A' is the constant and 'n' indices indirect (n = ½) or direct (n = 2) bandgap material. Also 'E_g' is bandgap energy, and 'λ' is wavelength corresponding to the absorption edge. A higher degradation rate is performed by lower bandgap material in general. The analysis results found that prepared composite MR-2 shows 2.8 eV which is lower than other materials such as 3.2 eV for both MR-1 and MnS_2 respectively (Fig.6). The higher degradation rate led by MR-2 composite due to the fabrication of MnS_2 on RGO layers which extent more species accommodate on the surface of the composite, it could be a promising photocatalyst for dye decolourisation.

Morphology study

The prepared samples were further examined for their structural morphology using transmission electron microscopy (TEM) analysis. The results are shown in Fig.8 which showed a great agglomeration with spherical in shape. However, the average particle size of prepared composite was found to be 26 nm is obtained from histogram distribution curve, is a bit higher compared to the results in XRD owing to the composite's multiple crystallinities [16]. Selected area electron diffraction (SAED) analysis contribution is great in determining the composite multiple crystallinity and very clear circular patterns were found from the XRD patterns, confirms the desirable compound is formed without any impurities.

UV-Visible spectrometer analysis is performed in this study to determine the optical properties of prepared MnS_2 and MnS_2-RGO composites (MR-1 and MR-2). Fig.7 displays the UV-Vis absorption spectra of prepared samples show the electrons excitation.

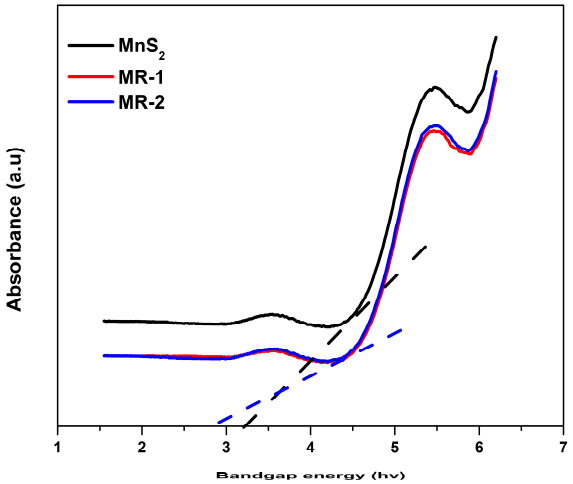

Figure 6: UV-DRS spectra of prepared samples

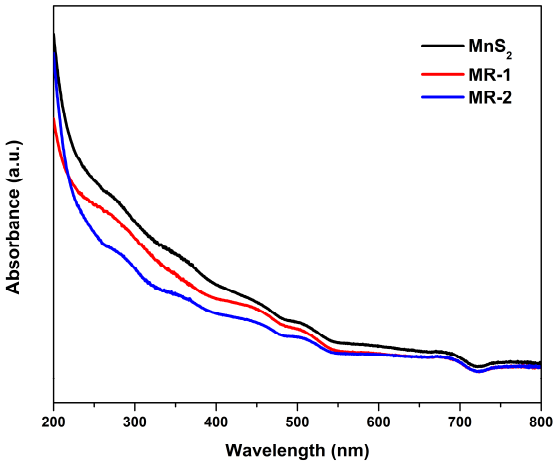

Figure 7: UV-Vis spectral analysis of prepared MnS_2 and MnS_2-RGO composites

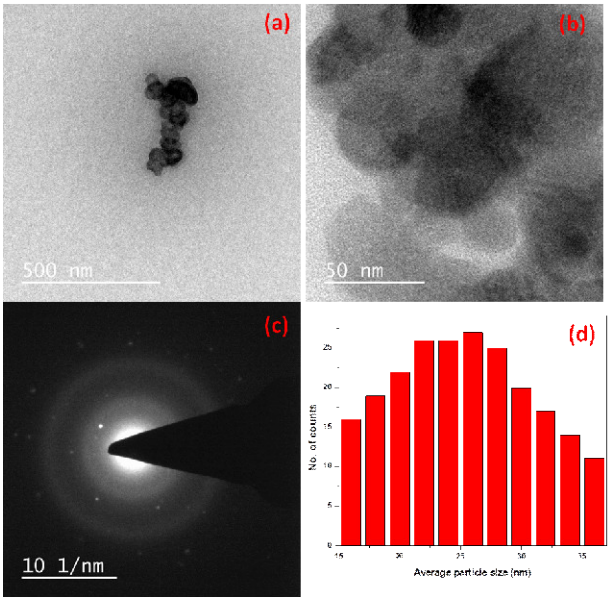

Figure 8: (a,b) TEM images, (c) SAED and (d) histogram distribution curve of prepared samples

Further morphology of prepared samples (MnS_2, MR-1 and MR-2 composites) *via* co-precipitation approach was studied by scanning electron microscopy (SEM) with the range of 1µm to 200 nm. Noticed that co-precipitation route approach favours the fine morphology of prepared samples are formed. Fig.9 interprets the SEM images of MnS_2 and composites which are in spherical shape with uniformity. Also noticed that, bare MnS_2 lies on the surface of layers of RGO that have reached out more aggregation as p-p interactions over RGO layers [4].

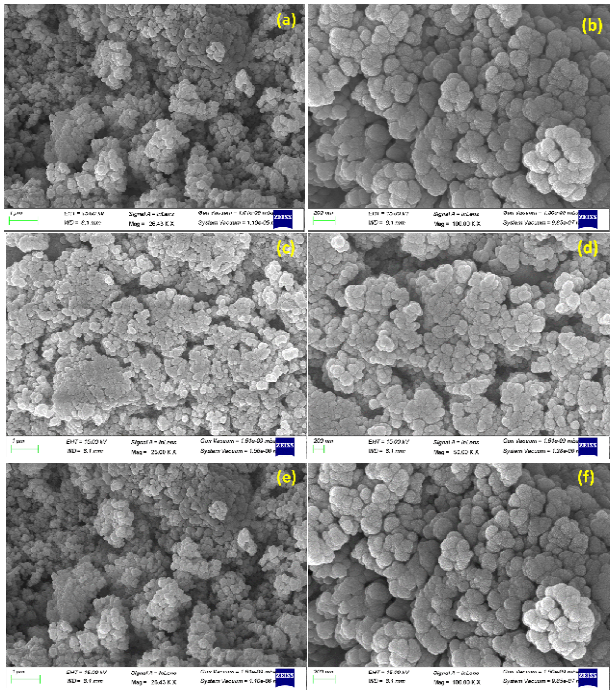

Figure 9: SEM micrographs of prepared (a,b) MnS_2, (c,d) MR-1 and (e,f) MR-2 composites

The elemental analysis of the prepared composite was studied using energy dispersive x-ray spectroscopy (EDX). Fig.10 exhibits the peaks of elements such as carbon (C), oxygen (O), Manganese (Mn) and sulphur (S) evident the purest form of MnS_2-RGO composite is formed with no impurities.

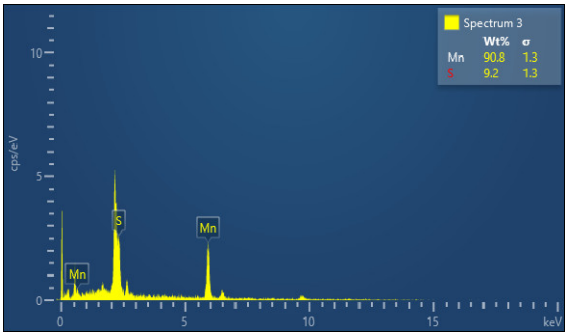

Figure10: EDX analaysis of prepared MnS_2

Photocatalytic degradation studies

The photocatalytic activity of synthesized MnS_2-RGO composite was studied in the degradation of *O*-Nitrophenol (ONP) organic pollutants under visible light illumination. Initially, the MnS_2 was tested under vigorous conditions such as 0.03g of catalyst and 10 ppm of dye solution which is alkaline based on literature and showed less degradation efficiency (91.73%). Later degradation of ONP was tested using hydrothermally prepared MnS_2-RGO composite under visible light irradiation and exhibited better results in degradation as shown in Fig.11. In order to optimize the experimental conditions such as the effect of pH, catalyst amount and dye concentration solution were also studied.

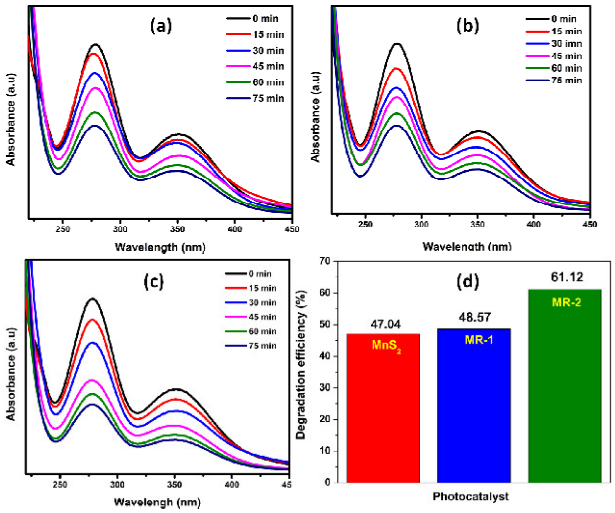

Figure 11: Photocatalytic degradation of *o*-nitrophenol using prepared (a) MnS_2, (b) MR-1, (c) MR-2 composites and (d) overall degradation efficiency

Effect of pH of dye solution

The role of pH plays a key factor in photocatalysis. In this study, three different pH such as 4, 7 and 10 were used to evaluate of photocatalytic activity of composite. Interestingly the maximum degradation efficiency was noticed at pH-10 under kept constant such as catalyst dose (0.01g) and initial dye concentration (10 ppm) of *o*-nitrophenol carried out. The degradation efficiencies of the composite are 59.28, 61.12and 91.73% at their respective pH-4, 7 and 10, shown in Fig.12. Furthermore, when the pH is greater than pH-10, the degradation of *o*-nitrophenol decreased with an increase in pH due to pH played a great role in photocatalysis. Hence, for better adsorption of the dye on the catalyst surface, the surface must be maintained the pH-10for degradation of *o*-nitrophenol solution by MnS_2-RGO composite.

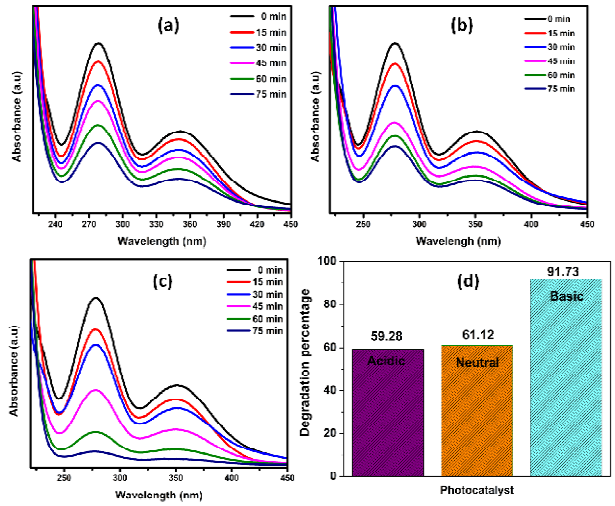

Figure12: Effect of pH on degradation of o-nitrophenol using MR-2 composite (a) acidic, (b) neutral, (c) basic and (d) overall degradation

Effect of Catalyst Dose

To study the effect of catalyst dosage on the degradation of *o*-nitrophenol, a series of experiments were conducted to get optimum catalyst loading by varying the selected catalyst dosage ranging from 0.01g and 0.02g at a fixed pH-10 and dye concentration (10 ppm) of *o*-nitrophenol aqueous solution. With the increase of catalyst dosage rate of degradation increases (0.02 g possess 96.93% but 0.01 g possess 91.73 Fig.13), since the active surface becomes constant, the number of photons absorbed and the number of dye molecules adsorbed is increased concerning an increase in the number of catalyst molecules.

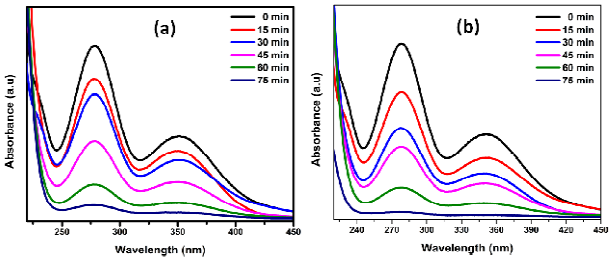

Figure 13: Effect of catalyst dosage on % degradation of *o*-nitrophenol by MR-2 composite loading amounts of (a) 10mg and (b) 20mg

Effect of Dye Initial Concentration

The effect of initial *o*-nitrophenol concentration on degradation using MnS_2-RGO composite is illustrated in Fig.14. The influence of the initial concentration of *o*-nitrophenol on the degradation rate was explored by varying the concentration to 10, 20 and 30 ppm at a fixed catalyst loading (50 mg) using an alkaline solution. Simultaneously, the degradation rate increased with dye concentration till 20 ppm, and the degradation rate decreased after increasing in excessive dye concentration. This may be due to the concentration of dye increase, more dye concentration will be available for excitation and energy transfer [4] which enhances the degradation percentage, but above the limit due to the fact that at the higher concentration dye start covering the active surface of photocatalyst as a blanket and intercepting from light intensity [15] that decreases degradation.

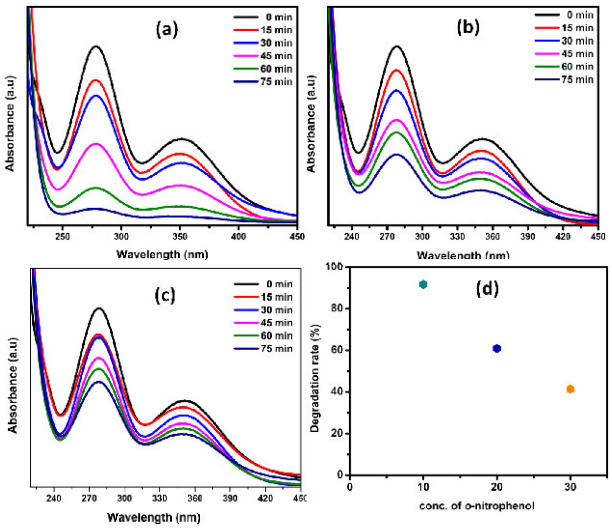

Figure 14: Effect of initial dye concentration on % degradation of *o*-nirophenol

The simulated visible light photoreaction of the *o*-nitrophenol dye solution with the selected nanocomposite shows relatively satisfactory results. But in the absence of nanocomposite, no dye degradation was observed. These rate values indicate the rate of degradation of *o*-nitrophenol in an alkaline medium. The optimized conditions for degradation of *o*-nitrophenol using MnS_2-RGO composite are 50mg catalyst loading, basic pH and initial concentration of 10 ppm of *o*-nitrophenol aqueous solution.

Proposed mechanism

A plausible mechanism of photocatalytic degradation performance of prepared MnS_2-RGO composite under visible light irradiations is schematically illustrated in Fig.15. The MnS_2-RGO nanocomposite is kept in visible light illumination; initially, MnS_2 undergoes a charge separation process that leads to the promotion of electrons from the valence band (VB) to the conduction band (CB) and leaving a hole in the VB. Due to the formation of heterojunction, the photogenerated electrons in CB of MnS_2 transferred to CB of MnS_2. Meanwhile, the excited holes at the valence band (VB) of MnS_2 were transferred to the VB of MnS_2. Finally, the photogenerated electrons are captured by the RGO sheets through semiconductor carbon heterojunction which dramatically enhanced photogenerated charge separation efficiency in MnS_2-RGO nanocomposite. Simultaneously an equal amount of holes have been formed in semiconductor nanocomposite. These separated electrons and holes directly react with oxygen and water to generate highly reactive superoxide radicals ($^{\bullet}O_2^-$) and hydroxyl radicals ($^{\bullet}OH$). These energetic reactive radicals consequently react with surface adsorbed nitrophenols molecules and degraded them into small intermediate molecules, such as CO_2 and H_2O. Based on the above mechanism explanation for photocatalytic degradation of dye in the presence of MnS_2-RGO nanocomposite under visible light irradiation was shown by the following equations (3-10).

$$MnS_2 + h\nu \longrightarrow MnS_2(e^-) + MnS_2(h^+) \quad (3)$$

$$MnS_2(h^+) + H_2O \rightarrow MnS_2 + {}^{\bullet}OH + H^+ \quad (4)$$

$$MnS_2(e^-) + RGO \rightarrow RGO(e^-) + MnS_2 \quad (5)$$

$$RGO(e^-) + O_2 \longrightarrow RGO + {}^{\bullet}O^-_2 \quad (6)$$

$$H_2O + {}^{\bullet}O^-_2 \longrightarrow HO_2{}^{\bullet} + OH^- \quad (7)$$

$$2HO_2{}^{\bullet} \longrightarrow H_2O_2 + O_2 \quad (8)$$

$$H_2O_2 + {}^{\bullet}O^-_2 \longrightarrow OH^- + {}^{\bullet}OH + O_2 \quad (9)$$

$$^{\bullet}OH/{}^{\bullet}O^-_2/\ HO_2{}^{\bullet} + dye \longrightarrow \text{Degradation products} \quad (10)$$

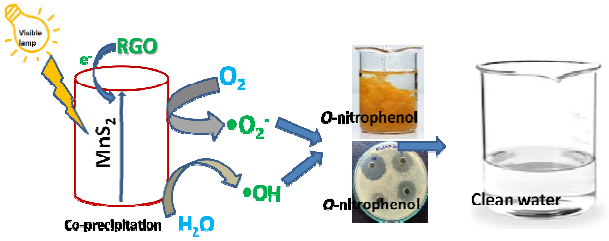

Figure 15: Photocatalytic degradation of dyes using MnS_2-RGO composite

The synthesized reduced graphene oxide based metal sulfide composite showed better photocatalytic activity due to increases in the number of impurity energy levels between the VB and CB which helps for the generation of more electron-hole pairs, thus decreasing the recombination of photogenerated holes and electrons by reduced graphene oxide [1-3] to eliminate the harmful effect of defect bands.

Recyclability and Sustainability

The prepared composite was further examined for its recyclability and stability towards the degradation of *ortho*-nitrophenol. In that sense, the used photocatalyst was collected after completion of the degradation experiment. The collected photocatalyst was washed thoroughly with water followed by the ethanol, centrifuged and finally dried for further degradation experiment. A remarkable degradation rate was achieved by reused photocatalyst, and the same experiment pursues up to six cycles. The degradation rate decreased gradually and reached 80 % at the sixth cycle due to the weight loss of photocatalyst during the washing (Fig.16). After recycling the photocatalyst, it is further examined for its sustainability by characterizing it with XRD. There is no change in the XRD planes of the tested photocatalyst, which means it is stable for up to six cycles as shown in Fig.17.

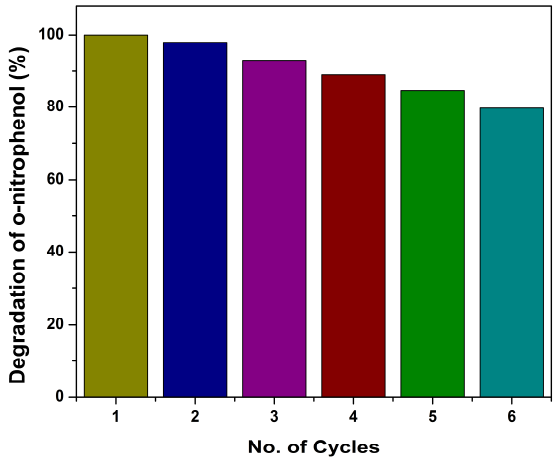

Figure 16: recyclability test of prepared MnS_2-RGO composite

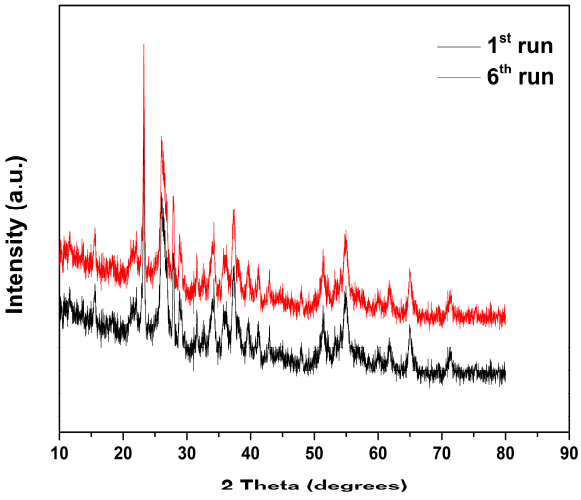

Figure 17: Sustainability of prepared MnS_2-RGO composite

Antimicrobial activity

The MnS_2-RGO composites and pure FeS_2 were tested with pathogens such as *E.coli*, *S.aureus, S.typhi and V.cholera*. Fig.18 describes the antimicrobial performance of prepared MnS_2 over the pathogens at the standard of Chloramphenicol. The obtained results found that less zone of inhibition was achieved. The maximum inhibition occurred by MR-2 composite than MR-1 composite over the tested pathogens as the insertion of RGO with FeS_2. Table 1 shows the zone of inhibition of tested samples on various microorganisms. The tested MR-2 composite exhibited a greater inhibitory effect recorded against *E.coli* (16 µg/mL) and gram-positive bacteria is observed (Fig.19) to be so effective than gram-negative. *S.typhi* exhibits greater inhibition of its growth rate using tested composites.

Table1: Zone of inhibition (mm) of prepared samples

Organism	MnS_2	MR-1	MR-2	Standard (µg/mL)
E.coli	13 ± 0.1	15 ± 0.4	16 ± 0.7	30 ± 0.6
S.aureus	10 ± 0.5	11 ± 0.2	12 ± 0.4	33 ± 0.2
S.typhi	11 ± 0.2	12 ± 0.7	15 ± 0.3	31± 0.5
V.cholera	10 ± 0.6	10 ± 0.1	11 ± 0.1	32 ± 0.1

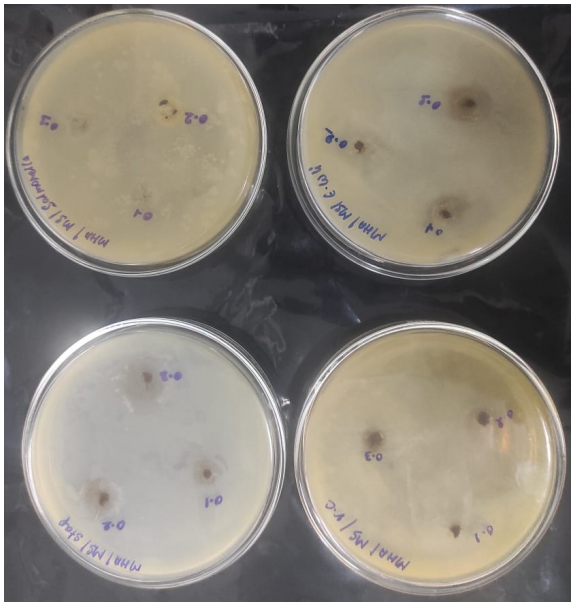

Figure 18: Antimicrobial activity of prepared MnS_2

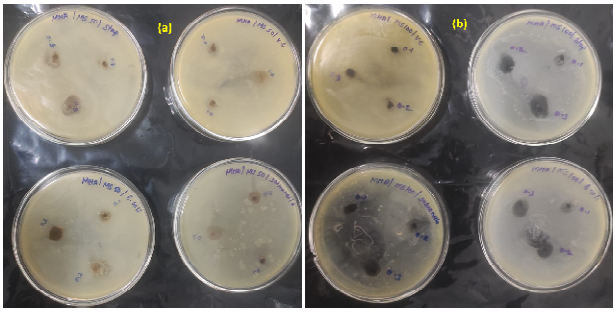

Figure 19: Antimicrobial activity of prepared MnS_2-RGO composites (a) MR-1 and (b) MR-2

Conclusions

Herein, we address water pollution and its causes mainly by nitrophenols and microorganisms. To overwhelm the solution, we prepared a composite with MnS_2 and RGO by co-precipitation approach. The prepared materials are well

confirmed with various sophisticated instruments and studied their physical, chemical and optical properties. The photocatalytic activity of prepared samples was executed by the photodegradation of nitrophenols under visible light irradiations. The results stated that prepared FR-1 composite shows lesser in size compared to other material which declares that MR-1 have a greater surface area that can accommodate more dye molecules on the surface. The MR-2 composite degraded nitrophenols completely in 180 min and the optimum conditions are studied in sense of pH, catalyst dose and dye concentration. The MnS_2-RGO composites and pure MnS_2 were tested with pathogens such as *E.coli, S.aureus, S.typhi and V.cholera*. Initially, the antimicrobial performance of prepared MnS_2 over the pathogens at the standard of Chloramphenicol was studied and found less zone of inhibition achieved. The maximum inhibition occurred by MR-2 composite than MR-1 composite over the tested pathogens as the insertion of RGO with MnS_2. Hence, a current composite can be applied to cleaning the wastewater on a large scale with cost-effective and eco-friendly.

References

1. Botsa, S.M., Basavaiah, K. Fabrication of multifunctional TANI/Cu_2O/Ag nanocomposite for environmental abatement, Sci Rep., 2020, 10, 14080.
2. G Ravi, M Sarasija, D Ayodhya , LS Kumari, D Ashok, Facile synthesis, characterization and enhanced catalytic reduction of 4-nitrophenol using NaBH4 by undoped and Sm3+, Gd3+, Hf3+ doped La2O3 nanoparticles, Nano Convergence, 2019, 6, 12.
3. AS Hashimi , MANM Nohan, SX Chin, S Zakaria, CH Chia, Rapid Catalytic Reduction of 4-Nitrophenol and Clock Reaction of Methylene Blue using Copper Nanowires, Nanomaterials, 2019, 9, 936.
4. GS Sree, SM Botsa, BJM Reddy, KVB Ranjitha. Enhanced UV–Visible triggered photocatalytic degradation of Brilliant green by reduced graphene oxide based NiO and CuO ternary nanocomposite and their antimicrobial activity, Arab J Chem., 2020, 13 (4), 5137-5150.
5. Yi M, Shen Z. A review on mechanical exfoliation for the scalable production of graphene, J Mater Chem A Mater Energy Sustain, 2015, 3, 11700-11715.
6. Yein WT, Wang Q, Feng X, Enhancement of photocatalytic performance in sonochemical synthesized ZnO–rGO nanocomposites owing to effective interfacial interaction, Environ Chem Lett, 2018, 16, 251–264.
7. Adeghi MH, Tofighy MA, Mohammadi T. One-dimensional graphene for efficient aqueous heavy metal adsorption: Rapid removal of arsenic and mercury ions by graphene oxide nanoribbons (GONRs), Chemosphere, 2020, 253, 126647.
8. Peng X, Mo S, Li R, Effective removal of the rare earth element dysprosium from wastewater with polyurethane sponge-supported graphene oxide–titanium phosphate, Environ Chem Lett, 2021, 19, 719–728.
9. N. Hebalkar, A. Lobo, S.R. Sainkar, W. Vogel, S.K. Kulkarni, Properties of zinc sulphide nanoparticles stabilized in silica, J. Mater. Sci, 2001, 36, 4377.
10. C. Sombuthawee, S.B. Bonsall, P.A. Humme, Phase equilibria in the systems ZnS⍰MnS, ZnS⍰CuInS2, and MnS⍰CuInS2, J. Solid State Chem, 1978, 25, 391.
11. Bayantong ARB, Shih YJ, Ong DC, Adsorptive removal of dye in wastewater by metal ferrite-enabled graphene oxide nanocomposites,Chemosphere, 2020, 274, 129518.
12. L. Samad, M. Cabán, Acevedo, M.J. Shearer, K. Park and R.J. Hamers, Ionization of High-Density Deep Donor Defect States Explains the Low Photovoltage of Iron Pyrite Single Crystals, Chem Mater, 2015, 27, 3108-3114
13. AG Raju, BD Rao, G Himabindu, BS Mohan, Iron Pyrite Thin Films Synthesized from an Fe(acac)3 Ink, J Mater Res Tech., 2022, 17, 2648-2656.
14. E. Bastola, KP Bhandari, RJ Ellingson, Application of composition controlled nickel-alloyed iron sulfide pyrite nanocrystal thin films as the hole transport layer in cadmium telluride solar cells, J.Mater.Chem.C, 2017, 5, 4996-5004.
15. GS Sree, BS Mohan, BJM Reddy, KVB Ranjitha, Deterioration of Cadmium and pathogens from contaminated water using hydrothermally prepared NiO-ZnO-RGO composite, J Mater Res Tech., 2021, 10, 976-987.
16. E. Bastola, K.P. Bhandari and R.J. Ellingson, Application of composition controlled nickel-alloyed iron sulfide pyrite nanocrystal thin films as the hole transport layer in cadmium telluride solar cells, J. Mater Chem C, 2017, 5, 4996-5004.